

The Heliosphere in Time

H.-R. Müller · P. C. Frisch · B. D. Fields · G. P.
Zank

Received: 15 April 2008 / Accepted: 30 September 2008

Abstract Because of the dynamic nature of the interstellar medium, the Sun should have encountered a variety of different interstellar environments in its lifetime. As the solar wind interacts with the surrounding interstellar medium to form a heliosphere, different heliosphere shapes, sizes, and particle contents result from the different environments. Some of the large possible interstellar parameter space (density, velocity, temperature) is explored here with the help of global heliosphere models, and the features in the resulting heliospheres are compared and discussed. The heliospheric size, expressed as distance of the nose of the heliopause to the Sun, is set by the solar wind - interstellar pressure balance, even for extreme cases. Other heliospheric boundary locations and neutral particle results correlate with the interstellar parameters as well. If the H⁰ clouds identified in the Millennium Arecibo survey are typical of clouds encountered by the Sun, then the Sun spends ~ 99.4% of the time in warm low density ISM, where the typical upwind heliosphere radii are up to two orders of magnitude larger than at present.

Keywords Global heliosphere modeling · time-dependent interstellar conditions

1 Introduction

The expansion of the coronal solar wind is terminated by encountering the interstellar material surrounding the solar system, the circum-heliospheric interstellar medium (CHISM).

To appear in Space Science Reviews, "From the Outer Heliosphere to the Local Bubble", J. Linsky et al. (eds); ISSI workshop held Oct. 2007

Hans-R. Müller
Department of Physics and Astronomy, Dartmouth College, Hanover, NH 03755, USA
Tel.: +1-603-6460428
E-mail: hans.mueller@dartmouth.edu

Priscilla C. Frisch
E-mail: frisch@oddjob.uchicago.edu

Brian D. Fields
E-mail: bdfields@uiuc.edu

Gary P. Zank
E-mail: zank@cspar.uah.edu

The Sun is currently embedded in partially ionized material, with about three fourths of the material in neutral form. Absorption studies toward nearby stars reveal a very inhomogeneous local interstellar medium, with many distinct velocity components in most lines of sight. Also on bigger scales, the ISM is a dynamic medium, constantly replenished and mixed anew by the outflows of star forming regions and supernova explosions, for example. Shock passages create large regions of almost empty, high-temperature regions in their wake which may be unstable and hence short-lived.

On its journey around the Galaxy, the Sun is likely to encounter a variety of such interstellar environments, each of which is characterized by a set of physical quantities, including density, temperature, magnetic field, and velocity state. As the solar wind is often assumed to have been relatively stable over long periods of time, the question arises how the heliosphere has reacted to the differing interstellar environments encountered through time. We characterize in this paper the heliospheric response to some non-catastrophic changes in the interstellar environment (“galactic weather”). Studies like this, paired with cosmic ray calculations and investigations of the terrestrial consequences of changes in the interplanetary medium due to galactic weather events, will contribute to the understanding of long-ago events that left their mark in terrestrial records.

A concrete example is the evidence that the relatively warm and dense material of the contemporary local interstellar cloud (LIC) is thought to be embedded in a larger structure, the Local Bubble (LB). With some reasonable assumptions, it can be estimated that the Sun was exposed to the tenuous, very hot LB environment for a long time, has only entered the LIC some 40,000 years ago, and will exit it in 0–4000 years from now. In this sense, roughly steady interstellar conditions are short-lived, and changes will occur on different time scales, with cloud passages as short as 10^3 years.

The variety of possible heliosphere boundary conditions that follow from our understanding of interstellar clouds dictate that diverse models of the heliosphere are required. The models must accommodate the extremes that the Sun may have encountered over time. For most of the discussion below we use a heliospheric multifluid model that self-consistently incorporates the charge-exchange interactions between interstellar neutral atoms and the solar wind. The dynamics of the solar wind, and therefore the heliosphere characteristics, are altered substantially by mass-loading from interstellar H° atoms, so modeling both the pristine and charge-exchange H is a key aspect of understanding variations in the heliosphere as the Sun passes through different galactic environments. These models form the basis for the discussions in Sections 2 and 4. For the extreme and short-lived interstellar environment experienced by the passage of an interstellar shock over the heliosphere, discussed in Section 3, we use a different model.

2 Basic Model Results

To investigate the influence of the interstellar conditions on the heliosphere, a detailed global heliospheric multifluid code is used that self-consistently calculates plasma components and neutral hydrogen (Pauls et al., 1995; Zank et al., 1996; Müller et al., 2006a). Its strength lies in the detailed treatment of the neutral component, which originates in the ISM but is out of equilibrium when passing through the heliosphere. This is the consequence of charge exchange where neutral atoms are lost to the plasma, and new neutrals are inserted into the distribution with velocity characteristics that represent the underlying plasma protons. Because the mean free paths can be quite long, the multifluid approach treats the neutrals

with three or four fluids, each representing the characteristic major different plasma regions where the respective secondary neutrals were born (e.g., Müller et al., 2008).

We first establish a detailed global heliospheric multifluid code that can accommodate the variable heliosphere boundary conditions that the Sun may have encountered over time. It assumes axisymmetry about the stagnation axis (the axis through the Sun that is parallel to the ISM flow) and an isotropic solar wind. The model grid is polar, with an inner inflow boundary at 1 AU (or even 0.7 AU for the smaller models of sections 2.3 and 2.4). There, the 1 AU solar wind parameters of 5.0 cm^{-3} for the plasma density, a temperature of 10^5 K , and a radial velocity of 400 km s^{-1} are used as standard values; they represent a typical in-ecliptic wind during solar minimum (slow solar wind). Each of the neutral fluids interacts with the plasma through resonant charge exchange, using the Fite et al. (1962) cross section, and all neutrals are subjected to photoionization which depends on the squared distance to the Sun. For simplicity, radiation pressure is assumed to balance gravity for neutral hydrogen, and heliospheric and interstellar magnetic fields are neglected. The interstellar medium is prescribed as inflow boundary condition at a suitably large distance from the interstellar bow shock (outer grid boundary at 500 AU for section 2.3, 800 AU for section 2.4, 1000 AU for section 2.1, and 1500 AU for section 2.2). The boundary parameters are the CHISM H^0 and H^+ number densities, and the (common) hydrogen velocity and temperature. Outflow boundary conditions are imposed on all fluids at the downwind outer boundary, and at the inner boundary for all neutral fluids. Photoionization already depletes the neutral density considerably there. Secondary neutrals are permitted to escape also through an outer outflow boundary condition in upwind directions.

2.1 Contemporary ISM (LIC)

As a proxy for the contemporary values of the CHISM boundary parameters we choose a model with $n(\text{H}^+) = 0.047 \text{ cm}^{-3}$, $n(\text{H}^0) = 0.216 \text{ cm}^{-3}$, $v = 26 \text{ km s}^{-1}$, and $T = 7000 \text{ K}$ (Slavin and Frisch, 2008). Figure 1 shows the plasma temperature (top panel) and density (bottom panel) along the stagnation axis as solid lines, together with the neutral H density (dash-dotted line). The heliospheric boundaries appear as discontinuities. The interstellar plasma goes through a bow shock (BS); the accompanying decreased speed communicates via charge exchange to the neutrals and creates a hydrogen wall (hydrogen overdensity; Baranov and Malama, 1993; Linsky and Wood, 1996) in the post-bow shock region. On the sunward side of the heliopause, the supersonic solar wind undergoes a termination shock (TS) transition, and the hot heliosheath plasma is diverted tailwards. Solar and interstellar plasma are separated by a contact discontinuity, the heliopause (HP). The thermodynamically distinct plasma regions (supersonic solar wind; hot heliosheath; interstellar plasma) define the characteristic heliospheric regions that form the basis of the multifluid treatment of the neutrals in the model.

Figure 1 also displays the temperature and density profile of a plasma-only model, corresponding to the Local Bubble environment (“LB”, dashed lines; presented in detail in section 2.2 below). It demonstrates that charge exchange is the source of solar wind heating from about 10 AU all the way to the TS: The “LIC”-model plasma temperature is monotonically increasing in this range, while the plasma-only model follows a strict adiabatic cooling. At the HP, charge exchange organizes an anomalous heat transport from solar heliosheath plasma to interstellar plasma; such an energy transport is absent in the “LB” case without neutrals (HP at 300 AU in Figure 1).

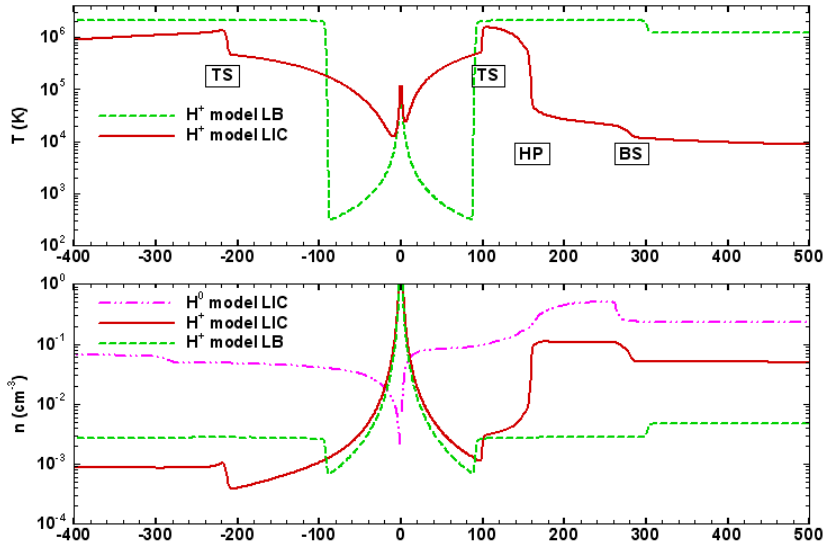


Fig. 1 One-dimensional profiles along the stagnation axis (distance in AU), with the Sun at center (0) and the CHISM coming from right. Top: plasma temperature of the Local Bubble case (dashed) and the contemporary conditions (solid). The heliospheric boundaries of the LIC model are marked in the plot. The bottom panel contains the corresponding densities (LB plasma model, dashed; LIC model: plasma, solid; neutral H, dash-dot pattern).

The neutral atom density at the upwind TS is $0.098 \text{ cm}^{-3} = 0.46 n(\text{H}^0)$. The factor 0.46 is called filtration factor, based on the image that the pristine interstellar neutral flow gets processed (“filtered”) while traversing the heliospheric interface between BS and TS (Wallis, 1971). Close to the Sun, photoionization and increased charge exchange probability (due to increased solar wind density) deplete neutral H exponentially, creating a neutral H cavity. In the tail direction, the stagnation axis re-populates slowly with off-axis neutral H.

2.2 Hot Local Bubble

The relative motions of the Sun and surrounding interstellar gas indicate the Sun has emerged from the deepest void of the Local Bubble interior within the past $\sim 130,000$ years. Such regions are common in the Milky Way Galaxy. Following this interpretation, the interior of this so-called Local Bubble is assumed hot and highly ionized but of low density. We adopt the ISM parameters of $n(\text{H}^+) = 0.005 \text{ cm}^{-3}$, $n(\text{H}^0) = 0$, $v = 13.4 \text{ km s}^{-1}$, and $\log T(\text{K}) = 6.1$ as a proxy model “LB” for such an interstellar environment, with the velocity based on the Dehnen and Binney (1998) solar apex motion since the LB plasma is assumed to be at rest in the Local Standard of Rest (LSR). The realization that part of the soft X-ray emission could be due to heliospheric foreground composed of line emission of solar wind charge exchange products being left in excited states, has recently cast doubt whether the Local Bubble gas is in fact as hot as stated above, so that the LB model outlined here can be taken as an upper limit.

The speed of sound in such a LB plasma is high, so that the solar movement through it is decidedly subsonic. In this case, there is no bow shock, and interstellar plasma gets decelerated adiabatically to match the zero velocity of the stagnation point. The isotropic thermal

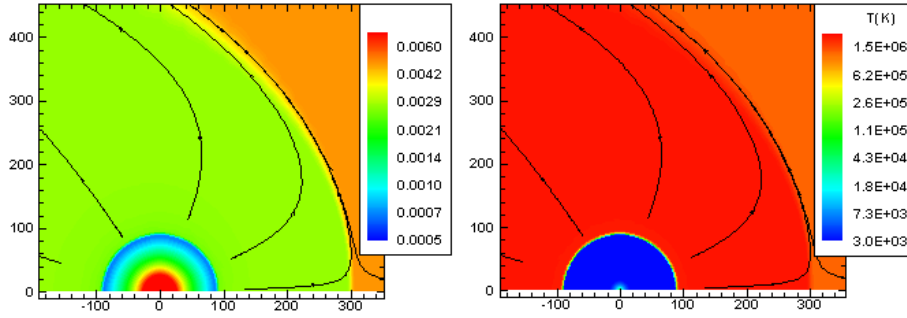


Fig. 2 Plasma density (left) and temperature (right) for the heliosphere surrounded by Local Bubble gas.

interstellar pressure dominates the ram pressure, and the termination shock is spherical at a distance of 90 AU from the Sun. This distance is comparable to that of the contemporary heliosphere. The distance to the nose of the heliopause is 300 AU, which makes the heliosheath very large in comparison to the one of the contemporary heliosphere. The temperature in the sheath reaches values as high as 2.2×10^6 K. Figure 2 shows 2D maps of density and temperature for the LB case, while Figure 1 contains both variables along the stagnation axis, as dashed lines. In the termination shock transition, the density jumps by a factor of 3.8, and the wind speed decreases to 100 km s^{-1} .

In the LB model there are no neutral atoms in the entire combined system of the solar wind and ISM. The result is that a host of physical effects present if neutral gas surrounds the Sun were missing when the Sun was in the LB: There are no pickup ions (PUI) produced by charge exchange, there are no anomalous cosmic rays, and no slowdown or heating in the supersonic solar wind beyond the inner solar system takes place. As mentioned by Müller et al. (2006a), the plasma-only LB model exhibits a morphology and flow field that are similar to the gross properties of the hydrodynamic problem of a flow around a rigid sphere (excluding the flow detachment and vortices occurring in the latter case). They also point to the fact that absent the mitigating effects of neutrals, the magnetic field of both solar and interstellar origin takes on a more important role in the pressure balance, and corrections to the above results can be expected when magnetic fields are included realistically.

2.3 Dense Neutral ISM

Müller et al. (2006a) have presented results from models with an ISM density that is about two orders of magnitude higher than the contemporary value. The resultant heliospheres are small because of the increased interstellar ram pressure shifting the pressure balance. The presence of a higher neutral density makes charge exchange a more frequent occurrence, so that the plasma slowdown at the BS gets immediately communicated to the neutrals with a resulting hydrogen wall that is sharply defined post-BS, and has a high amplitude. Although filtration is very effective, enough neutral hydrogen enters the inner heliosphere inside the TS to lead to a pronounced solar wind slowdown (values down to 260 km s^{-1} upstream of the TS) and heating; the TS itself is therefore quite weak even in the nose direction. The BS compression ratio, on the other hand, is somewhat elevated. Atypically, the HP is not a sharp temperature transition as in most other models, but the temperature profile is more gradual,

with the solar wind cooled close to the HP by frequent charge exchange, and the interstellar plasma heated close to the HP.

Even denser clouds encountering the heliosphere have been treated by Yeghikyan and Fahr (2003), with $n_{\text{tot}} = 100 \text{ cm}^{-3}$ and higher. Statistically such clouds could be encountered once every ~ 10 Myrs, once per Gyr for giant molecular clouds (cold, 10K, with up to 1000 cm^{-3} density). Not only does the heliosphere become extremely small for the duration of the encounter, such that most of the Earth orbit is in the ISM, but the presence of massive amounts of neutral hydrogen makes it necessary to include additional physics. For example, the interplanetary medium will no longer be optically thin, as is a good assumption for contemporary conditions. One important terrestrial consequence is that the high density leads to removal of terrestrial atmospheric oxygen, and other atmospheric effects (Yeghikyan and Fahr, 2004).

2.4 High Velocity ISM

Similarly to density, it is also worthwhile to explore variations in the relative Sun-ISM speed. The interstellar velocity V is a key variable in understanding the ISM-heliosphere interactions because the ram pressure varies as V^2 . As noted above, if the ISM is at rest with respect to the Local Standard of Rest, relative velocities of about 13 km s^{-1} result from the motion of the Sun in that frame of reference. In the contemporary case, the LIC moves with respect to the LSR, resulting in an overall 26 km s^{-1} relative motion. In addition, warm and cold H^0 clouds have radial velocities that vary from -80 to $+6 \text{ km s}^{-1}$, with the possibility that 3D velocities are even larger. For the purpose of calculating astrospheres around stars in the solar neighborhood that are still embedded in a partially ionized ISM, Wood et al. (2003, 2005) determine relative Star-ISM velocities for selected objects. In their list there are entries with 68 and 86 km s^{-1} , and 40 Eri has a relative motion of 127 km s^{-1} (Wood et al., 2003). When applying such relative motions to the Sun, the resulting heliospheres can be described as “wind-swept,” i.e., a narrow leading cavity and a long, drawn-out tail (Müller et al., 2006a). The high velocity generates a large ram pressure, making the resulting heliosphere smaller, similar to, but more elongated than, the high density cases. Such heliospheres also tend to have a triple point at the heliotail termination shock, necessitated by the heliosheath flow accelerating to supersonic velocities (e.g., Pauls and Zank, 1996).

Not only are the high-speed heliospheres quite asymmetric, but the neutral mean free paths are now on the order of the heliosheath thickness or larger, meaning that the hydrogen wall is not very pronounced, and neutral filtration is very weak so that the interstellar density is not much higher than the neutral density entering the inner heliosphere through the termination shock. Such filtration ratios close to 1 seem only possible when a high interstellar velocity combines with a modest or low density so that the peak hydrogen wall occurs close to the HP without room for depletion of neutral H between peak and HP.

3 Supernova Remnant Encounters with the Heliosphere

The possibility that spikes in ^{10}Be isotopes in the Antarctic ice core samples were caused by a cosmic-ray enhancement due to a supernova shock passing over the heliosphere was evaluated by Sonett et al. (1987). Initial supernova remnant (SNR) expansion velocities are much larger than the high-velocity cases discussed in section 2.4. Fields et al. (2008) have

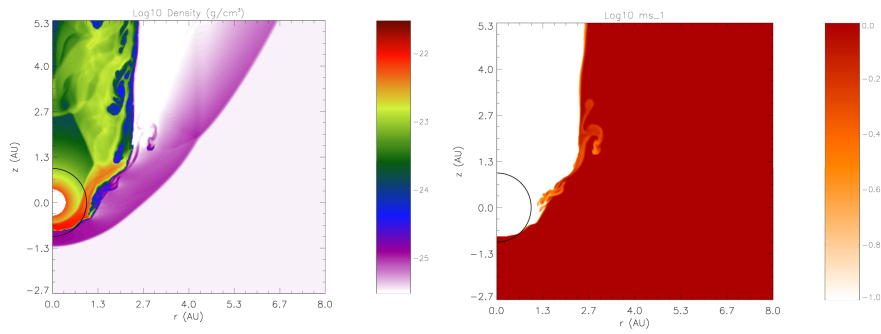


Fig. 3 (Left) Snapshot (logarithmic density map) of the heliosphere during arrival of a shock from a supernova explosion 8 pc away, for LIC-like ambient ISM conditions (the SNR velocity is $12,000 \text{ km s}^{-1}$). A circle is drawn at a radius of 1 AU indicating the Earth's orbit (modulo inclination effects). For a period of slow solar wind, a SNR under these conditions will engulf the Earth, and the Earth's orbit may carry it into the remnant where it will be directly exposed to supernova material. (Right) Corresponding contamination map ($C = 1$ supernova material, $C = 0$ solar material). Supernova material penetrates to 1 AU; solar wind and SNR plasmas mix also through instabilities at the heliopause.

recently calculated the effect on the heliosphere of a supernova going off in the solar neighborhood. One of the primary motivations of such studies is the evidence of live radioisotopes in thin layers of ocean floors with lifetimes shorter than the age of the solar system (Knie et al., 1999, 2004). A plausible explanation of such data is that a SNR collision with Earth has deposited this material (^{60}Fe) in a short-duration event (2.8 ± 0.4) Myr ago.

The effects of a SNR collision with the heliosphere depend on many factors, starting with the initial explosive energy, the density of the interstellar medium into which the supernova explodes, and the supernova distance. SNR shock front density, pressure, and velocity decrease with increasing distance from the supernova. Fields et al. (2008) have investigated a variety of ISM density parameters and distances, and modeled the SNR evolution from source to heliosphere with an AMR numerical code (FLASH; Fryxell et al., 2000); neutrals are neglected. Figure 3 displays an example of a heliosphere encountering a SNR from a 10^{51} erg supernova explosion at a distance of 8 pc, where the intervening ISM was assumed to have densities similar to the Local Bubble. This distance corresponds to the recent and conservative Gehrels et al. (2003) estimate for the limit at which the ionizing radiation from a supernova (prompt UV, X- and gamma-ray photons, as well as the later diffusive cosmic rays) inflicts damage on terrestrial stratospheric ozone at a level which can cause severe damage to the biosphere.

The passage of the supernova blast profile persists for thousands of years, with a slow secular decrease in pressure, velocity, and density. Consequently, high-speed, dense material comprises an interstellar wind on time scales of many solar cycles, such that on scales of the heliosphere the SNR blast is a basically steady, plane-parallel ISM wind. The snapshot in Figure 3 is taken with solar wind conditions reflecting solar minimum. It can be seen that the heliosphere is severely compressed, and the Earth orbit (black circle) dips into the shocked interstellar medium for part of the year, providing an interplanetary medium rich in supernova ejecta that might eventually precipitate to Earth to form the mentioned ocean bottom sediment layer. We see that an event close enough to cause biological damage is also able to deliver supernova debris to the Earth, raising the possibility that isotopic signatures can be correlated with possible supernova-induced mass extinctions.

4 Sensitivity of the Heliosphere to ISM Conditions

Utilizing a broad set of plausible interstellar boundary conditions for the heliosphere, it is possible to establish some correlations between such parameters and the resultant heliosphere configuration. To establish these correlations, numerous multi-fluid models of the heliosphere and astrospheres have been analyzed together. The models span the low-to-high interstellar velocities and densities of Müller et al. (2006a), with most of them obeying $500 < P/k < 6000 \text{ cm}^{-3}\text{K}$, and a study with values probing parameter space around the contemporary CHISM parameters with a similar range of P/k (see Müller et al. (2006b) for preliminary results). Regarding the latter study, the inferred values of the contemporary CHISM are $v = 26.3 \text{ km s}^{-1}$ and $T \sim 6300 \pm 340 \text{ K}$ (Witte et al., 1996; Möbius et al., 2004; Witte, 2004). The contemporary interstellar proton and neutral H densities are not well constrained but should lie in the range from $0.04\text{--}0.14 \text{ cm}^{-3}$ and $0.14\text{--}0.24 \text{ cm}^{-3}$, respectively (e.g. Zank, 1999; Slavin and Frisch, 2002). The setup for the systematic parameter study was therefore to probe the distinct densities of 0.05, 0.11, 0.17, and 0.23 cm^{-3} for both the interstellar neutral and plasma densities (16 combinations). The CHISM ionization fraction ranges from 18% to 82%. To explore the effects of temperature, it was decided to probe four temperatures 4000, 6000, 8000, and 10000 K, for a total of 64 models. The velocity in this parameter study was set to 26.24 km s^{-1} .

One result from the parameter study as well as from the extension to a wider parameter space is the predictability of the distance of the upwind heliopause (stagnation point) as an expression of the pressure balance between interstellar and solar wind. The HP distance is calculated from the Rankine-Hugoniot termination shock transition conditions and treating the heliosheath and shocked interstellar flows as incompressible (Suess and Nerney, 1990; Zank, 1999; Müller et al., 2006a). A relation is obtained that links the solar wind ram pressure $P_1 = \rho_1 v_{SW}^2$ at 1 AU and its scaling with heliocentric distance, to the interstellar total pressure P_{ISM} . In a supersonic case, the latter is dominated by $\rho_{ISM} v_{ISM}^2$ with $\rho_{ISM} = m_p [n(\text{HI}) + n(\text{HII})]$. The resulting heliopause distance takes the form

$$r_{HP} = r_0 \sqrt{\frac{\rho_1 v_{SW}^2}{P_{ISM}}} \left(1 - \frac{v_{ISM}^2}{v_{SW}^2} \right)^{\frac{5}{4}}. \quad (1)$$

The constant r_0 is a product of factors from the theoretical calculation and from the empirical fact that neutral hydrogen does not fully participate in the pressure balance, but only weakly couples to the plasma through charge exchange. A fit between model results and r_{HP} values yields a value of $r_0 = 1.70 \text{ AU}$, with about a 6% accuracy. A similar distance law was obeyed even by the high-velocity models of Fields et al. (2008) which represent SNR collisions with the heliosphere (section 3). Baranov et al. (1979) have studied analytically the plasma-only case without neutrals and arrive at a distance relation similar to equation (1), without the last factor (typically close to unity) involving the velocity ratio. Because of the entire ram pressure $P_{ISM} = \rho_{p,ISM} v_{ISM}^2$ participating fully in the pressure balance in this case, they arrive at a lower $r_0 = 1.4 \text{ AU}$, and the plasma-only heliospheric boundaries scale self-similarly with the factor $(\rho_1 v_{SW}^2 / \rho_{p,ISM} v_{ISM}^2)^{1/2}$.

The magnetic fields of solar and interstellar origin are neglected here; models that include interplanetary and interstellar magnetic fields are presented elsewhere (see for example the Opher contribution in this volume). It can be reasonably expected that for models with neutrals and magnetic fields, the inclusion of magnetic pressure in the pressure balance (1) will preserve its validity to some extent. However, most sensible interstellar magnetic

field configurations render the heliosphere asymmetric, and the distances of the boundaries as a function of direction become more complicated than equations (1)-(3) suggest.

In all available (non-magnetic) models, the nose distance of the heliopause is accurately coupled to the termination shock distance,

$$r_{\text{HP}} = (1.40 \pm 0.03) r_{\text{TS}}. \quad (2)$$

Again, this relation holds for SNR-type velocities as well (Fields et al., 2008, Figure 7). For the contemporary heliosphere, this result means that if the termination shock lies between 86 and 94 AU, the heliosheath in upwind direction is between 35 and 38 AU thick, for a heliopause distance between 121 and 132 AU.

The interstellar bow shock distance also correlates with the termination shock distance; however, there is an additional temperature dependence. For a higher interstellar temperature, the Mach number of the interstellar flow is lower, and hence the bow shock itself weaker. To still achieve a zero velocity at the stagnation point at the heliopause, the bow shock hence must be further out for higher temperatures, in spite of the higher interstellar pressure contributing to a slight shrinking of the overall heliospheric size. Multiplying a linear correlation with an ad-hoc term that grows for increasing temperatures gives a very good correlation between termination shock and bow shock distance,

$$r_{\text{BS}} = 1.5 r_{\text{TS}} \left(1 + \frac{1}{M-1} \right) + 23\text{AU} \quad (3)$$

(Müller et al., 2006b).

The shape of the termination shock is not spherical, but it is elongated in the tail directions. Typical values of the downwind/upwind ratio range between 2 and 3. The tail TS distance correlates with the upwind TS distance; however, there is again a temperature influence in this correlation. The higher the interstellar temperature, the lower the asymmetry of the TS between downwind and upwind direction. Empirically there is a correlation between $r_{\text{TS}}(180^\circ)$ and the quantity $r_{\text{TS}}(0^\circ)\sqrt{M}$, with a weak dependence of the proportionality factor on the interstellar neutral hydrogen density.

These results have been obtained from models where neutral hydrogen was present and influenced the plasma via charge exchange. The neutral hydrogen reaction to the different interstellar environments resists categorization more than is the case for the plasma results. For the 64-model systematic study, the height of the hydrogen wall (the peak neutral density between BS and HP) correlates with the interstellar Mach number. The higher the Mach number, the higher the resulting hydrogen wall. An expected anticorrelation between hydrogen wall height and amount of neutral hydrogen entering through the termination shock into the inner heliosphere could not be confirmed. There is, however, an anticorrelation of this filtration factor f with the interstellar plasma density, $f \propto 1/\sqrt[3]{n(\text{HII})}$.

5 Paleo-Heliosphere

The Arecibo Millennium Survey of the radio H^0 sky (Heiles and Troland, 2005) provides reliable statistics on the distribution of the column densities and velocities of warm and cold interstellar clouds seen from the tropical sky. About 60% of interstellar H^0 is warm neutral material (WNM). The median column density of the WNM, $1.3 \times 10^{20} \text{ cm}^{-2}$, exceeds that of CNM, $0.5 \times 10^{20} \text{ cm}^{-2}$ (Frisch, 2008). Although WNM is less dense than CNM, higher typical WNM velocities and column densities indicate that the Sun will spend more time in

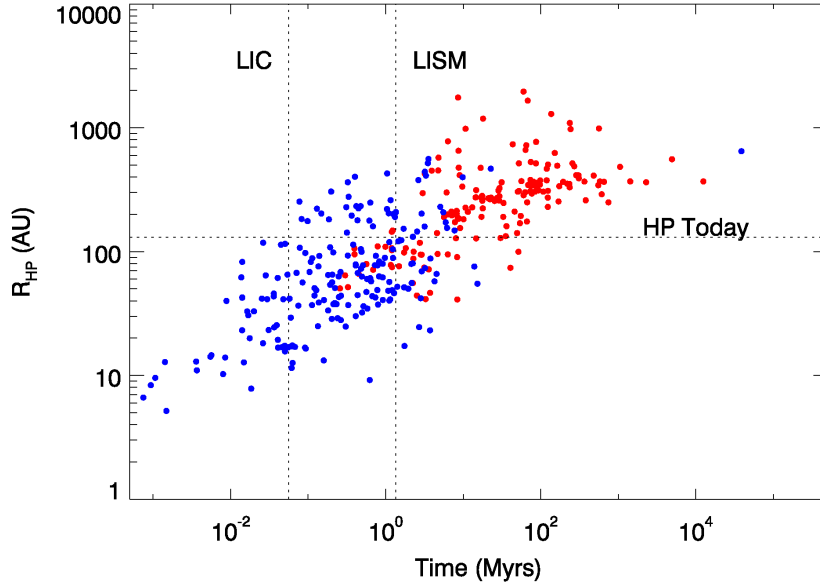


Fig. 4 The heliosphere in time, according to the tropical skies. The length of time, in Myrs, that the Sun would spend in the cold neutral (CNM) and warm neutral or partially ionized (WNM) interstellar clouds detected in the Arecibo Millennium Survey is plotted against the heliosphere radius predicted by eq. (1) for those clouds. The CNM clouds (blue dots) assume densities of 15 cm^{-3} , and the WNM clouds (red dots) assume densities of 0.27 cm^{-3} . The length of times that the Sun spends in the LIC, and in the very local interstellar material (LISM) is indicated, as is the present heliopause distance in the upwind. Since the true three-dimensional velocity of these clouds is unknown, this comparison assumes that the relative Sun-cloud velocity is the LSR velocity of each component detected by Arecibo. This plot shows that if the Arecibo sky samples ISM that is typical of that encountered by the Sun, then the Earth and Sun spends 99.4% of the time in WNM clouds.

the WNM than the CNM. We calculate the length of time that the Sun would be in each H^0 component detected in the Arecibo survey, and compare that time with the heliopause radius calculated from equation (1). We use assumed densities of 0.27 cm^{-3} and 15 cm^{-3} for the WNM and CNM, respectively, and assume that the observed LSR radial velocity for each component is typical of the encounter velocity. These values then give us a good estimate of the total length of time the Sun is likely to spend in WNM versus CNM interstellar gas. From Fig. 4 we quickly see that the Sun spends significantly more time in WNM than CNM types of clouds. According to the tropical Arecibo sky, the Sun is in WNM 99.4% of the time, but this estimate does not include the times spent in fully ionized regions. The Sun has entered the LIC within the past ~ 0.056 Myrs, and the LISM within the past ~ 0.13 Myrs, according to UV absorption lines towards nearby stars (Frisch and Slavin, 2006).

6 Conclusions

The ISM is a very dynamic environment. During its 5 Gyrs galactic trajectory, the solar system likely has been embedded in a wide variety of different interstellar environments. Some of these environments lead to a drastically reduced heliosphere size, allowing direct

access of interstellar material to the solar system and Earth. Even without direct ISM access, the particle flux background like cosmic rays and dust is sensitive to the ISM environment. The passage of the solar system through an arm of the galaxy likely triggers a pronounced increase of both the rate of supernovae going off near the Sun, and the flux of galactic cosmic rays. Consequences for the terrestrial atmosphere/climate, and their geological records, are likely (e.g., Frisch, 2006), but not part of this paper.

When calculating the heliosphere while including the interstellar neutrals self-consistently, and probing the vast interstellar parameter space, it can be confirmed that the overall heliospheric size is set by a pressure balance between solar wind and interstellar medium, with only weak modifications involving the interstellar Mach number and velocity (and most likely the magnetic pressure which was not included in this present analysis). The termination shock, heliopause, bow shock, and downwind termination shock locations exhibit simple correlations to the location of pressure balance. Neutral results like the filtration by the heliospheric interface, and the height of the hydrogen wall, also show a dependence on the interstellar parameters. For an encounter with dense ISM or very fast ISM, particle fluxes like neutrals, cosmic rays, and dust increase markedly at Earth orbit. A passage of a remnant of a nearby supernova blast has the ability to compress the heliosphere to a size that allows interstellar material including supernova ejecta direct access to Earth. In contrast, during the passage of the Sun through the Local Bubble, or through any almost completely ionized region, neutrals, pickup ions, and anomalous cosmic rays were entirely absent.

Acknowledgements HRM and PCF thank the International Space Science Institute (ISSI), Bern, Switzerland, for hosting the 2007 workshop “From the Heliosphere to the Local Bubble” and partially funding participation. HRM acknowledges partial funding through NSF grant AST-0607641 and NASA SHP grants NNG06GD48G and NNG06GD55G. PCF acknowledges funding through NASA grants NAG5-13107 and NNG05GD36G. The work of BDF was supported by NASA Exobiology grant EXB03-0000-0031.

References

- V. B. Baranov, M. G. Lebedev, M. S. Ruderman, *Astrophys. Space Sci.* **66**, 441–451 (1979)
- V. B. Baranov, Y. G. Malama, *J. Geophys. Res.* **98**, 15,157 (1993)
- W. Dehnen, J. J. Binney, *MNRAS* **298**, 387–394 (1998)
- B. D. Fields, T. Athanassiadou, S. R. Johnson, *Astrophys. J.* **678**, 549–562 (2008)
- W. Fite, A. Smith, R. Stebbings, *Proc. R. Soc. London Ser. A* **268**, 527 (1962)
- P. C. Frisch, *Solar Journey: The Significance of Our Galactic Environment for the Heliosphere and Earth* (Springer, Dordrecht, Netherlands, 2006)
- P. C. Frisch, *Space Sci. Rev.* (this volume), arXiv:0804.3798 (2008)
- P. C. Frisch, J. D. Slavin, *Astrophysics and Space Sciences Transactions* **2**, 53–61 (2006)
- B. Fryxell, K. Olson, P. Ricker, F. X. Timmes, M. Zingale, D. Q. Lamb, P. MacNeice, R. Rosner, J. W. Truran, H. Tufo, *Astrophys. J. Supp.* **131**, 273 (2000)
- N. Gehrels, C. M. Laird, C. H. Jackman, J. K. Cannizzo, B. J. Mattson, W. Chen, *Astrophys. J.* **585**, 1169 (2003)
- C. Heiles, T. H. Troland, *Astrophys. J.* **624**, 773–793 (2005)
- K. Knie, G. Korschinek, T. Faestermann, E. A. Dorfi, G. Rugel, C. Wallner, *Phys. Rev. Lett.* **93**, 171,103 (2004)
- K. Knie, G. Korschinek, T. Faestermann, C. Wallner, J. Scholten, W. Hillebrandt, *Phys. Rev. Lett.* **83**, 18 (1999)
- J. Linsky, B. Wood, *ApJ* **463**, 254 (1996)
- E. Möbius, M. Bzowski, S. Chalov, H.-J. Fahr, G. Gloeckler, V. Izmodenov, R. Kallenbach, R. Lallement, D. McMullin, H. Noda, M. Oka, A. Pauluhn, J. Raymond, D. Ruciński, R. Skoug, T. Terasawa, W. Thompson, J. Vallerger, R. von Steiger, M. Witte, *Astr. Astrophys.* **426**, 897–907 (2004)
- H.-R. Müller, V. Florinski, J. Heerikhuisen, V. V. Izmodenov, K. Scherer, D. B. Alexashov, H.-J. Fahr, *Astr. Astrophys.* (in press), doi: 10.1051/0004-6361:20078708 (2008)

-
- H.-R. Müller, P. C. Frisch, V. Florinski, G. P. Zank, *Astrophys. J.* **647**, 1491 (2006a)
- H.-R. Müller, G. P. Zank, P. Faurot-Pigeon, V. Jiwariyavej, R. Mutiso, F. Shafi, In *AIP Conf. Proc. 858: Physics of the Inner Heliosheath*, edited by J. Heerikhuisen, V. Florinski, G. P. Zank, N. V. Pogorelov, pages 33–38 (2006b)
- H. L. Pauls, G. P. Zank, *J. Geophys. Res.* **101**, 17,081–17,092 (1996)
- H. L. Pauls, G. P. Zank, L. L. Williams, *J. Geophys. Res.* **100**, 21,595 (1995)
- J. D. Slavin, P. C. Frisch, *Astrophys. J.* **565**, 364–379 (2002)
- J. D. Slavin, P. C. Frisch, *Astr. Astrophys.* (in press), doi: 10.1051/0004-6361:20078101 (2008)
- C. P. Sonett, G. E. Morfill, J. R. Jokipii, *Nature* **330**, 458 (1987)
- S. T. Suess, S. Nerney, *J. Geophys. Res.* **95**, 6403–6412 (1990)
- M. K. Wallis, *Nature* **254**, 202–203 (1971)
- M. Witte, *Astron. Astrophys.* **426**, 835–844 (2004)
- M. Witte, M. Banaszkiwicz, H. Rosenbauer, *Space Sci. Rev.* **78**, 289 (1996)
- B. Wood, J. Linsky, H.-R. Müller, G. Zank, *Astrophys. J.* **591**, 1210–1219 (2003)
- B. Wood, H.-R. Müller, G. Zank, J. Linsky, S. Redfield, *Astrophys. J. Lett.* **628**, L143–L146 (2005)
- A. Yeghikyan, H. Fahr, *Annales Geophys.* **21**, 1263–1273 (2003)
- A. Yeghikyan, H. Fahr, *Astr. Astrophys.* **425**, 1113–1118 (2004)
- G. P. Zank, *Space Sci. Rev.* **89**, 413–688 (1999)
- G. P. Zank, H. L. Pauls, L. L. Williams, D. T. Hall, *J. Geophys. Res.* **101**, 21,639 (1996)